ISBN: 978-3-95450-132-8 doi:10.18429/JACoW-IPAC2014-THPME150

SPECTROMETER FOR SRF GUN

I.Yu. Vladimirov#, V.I. Shvedunov, MSU, Moscow, Russia
T. Kamps, J. Voelker, HZB, Berlin, Germany

Abstract

We report about the design of a spectrometer for energy spectrum measurement of an electron beam generated by a superconducting radio-frequency photoelectron gun (SRF gun), which is under construction at HZB for bERLinPro. The spectrometer shall provide energy resolution about 0.1%. The spectrometer will be also used for single shot phase space measurements in combination with a transverse deflecting cavity (TCav).

INTRODUCTION

The spectrometer described in this report will be used for beam parameters measurements of SRF gun being developed in framework of GunLab [1] which is part of bERLinPro [2] of Helmholtz-Zentrum Berlin for Materials and Energy research (HZB).

bERLinPro is designed to develop and to demonstrate the CW linac technology and expertise required to drive next-generation accelerator facilities that are based on energy recovery linac principle.

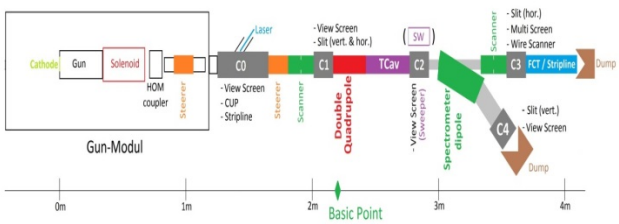

Figure 1: GunLab beamline.

GunLab is the research and development platform for SRF photoinjectors of bERLinPro. Fig. 1 shows a scheme of the beam diagnostic line in experiment GunLab. The spectrometer (Spectrometer dipole in Fig. 1) described in this report will be situated in GunLab beamline to measure energy and energy spectrum of the electron beam. Together with a TCav the spectrometer will be used to measure longitudinal phase space of a single bunch.

SPECTROMETER PARAMETERS

Scheme of the spectrometer is shown in Fig. 2. The spectrometer consists of two drift sections, dipole magnet and YAG-screen. During optimization the spectrometer was characterized by the next parameters: $L1$ and $L2$ – lengths of first and second drift sections; R and φ – bending radius and angle; θ – angle of pole face rotation; G – gap height of magnet; $K1$ – fringe field coefficient.

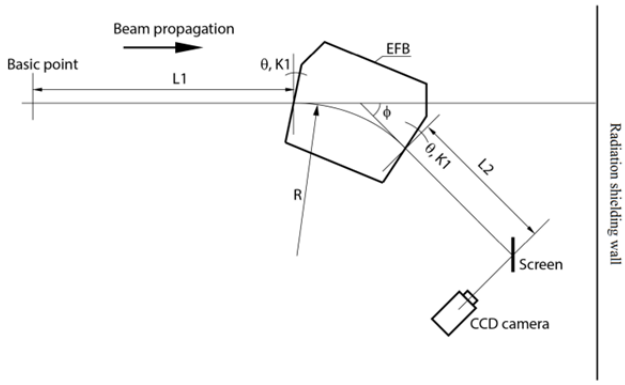

Figure 2: Scheme of the spectrometer.

The next requirements were imposed on the spectrometer design. The spectrometer must be configured to measure the energy and energy spectrum of electron beam in the energy range $1 \le E \le 10$ MeV with rms energy resolution $\Delta\delta$ better than 0.1%. The dipole magnet must occupy less than 40 cm in the beam line and its aperture must be $G > 30$ mm. The first drift section length $L1$ must be large enough ($L1 > 60$ cm) in order to incorporate a TCav. Vertical plane beam optics of the spectrometer must be optimized taking into account necessity of phase space measurements with TCav.

The resolution of the spectrometer is limited first of all by transverse beam emittance. To get high energy resolution we install collimating slit with width $2s$ at Basic point (Fig. 2) and optimize 6×6 transformation matrix from Basic point to the screen so that $m_{12} = 0$. In this case in the first order the energy resolution is defined by $\Delta\delta_\epsilon \le \frac{|m_{11}|}{m_{16}} s$.

Optimal parameters of the spectrometer are given in Table 1. Required energy resolution ($\Delta\delta_\epsilon \le 0.1\%$) is achieved with $2s = 1$ mm collimation slit.

Table 1: Optimal Spectrometer Parameters

Parameter	Value	Parameter	Value
G	35 mm	φ	45°
$L1$	800 mm	θ	7.593°
$L2$	1000 mm	$K1$	0.3
R	250 mm		

DIPOLE SIMULATION

3D dipole simulation was done with CST code [3]. Figs. 3 (a, b) show half of the dipole and distribution of magnetic induction along the reference trajectory within the dipole. With passive screens at magnet entrance and exit we provide $K1 = 0.28$.

The calculated 3D field map was implemented in ASTRA [4] to calculate the dynamics of the electron

#timerke@mail.ru

ISBN: 978-3-95450-132-8 doi:10.18429/JACoW-IPAC2014-THPME150

beam in the spectrometer. Different 6D phase space beam distributions at Basic point for this simulation were taken from SRF gun simulation. Example of simulation for electron beam with average momentum $\langle p \rangle = 3.060$ MeV/c and momentum spread $\frac{\Delta p}{p} = 0.0013$ is given in Fig. 4 (blue points). The rms beam size at the screen is $\Delta x = 0.99$ mm. To demonstrate that this value is dominated by the energy spread, we also simulated the same initial distribution without energy spread $\Delta p = 0$ eV/c. The resulting distribution on the screen is plotted as black points in Fig. 4.

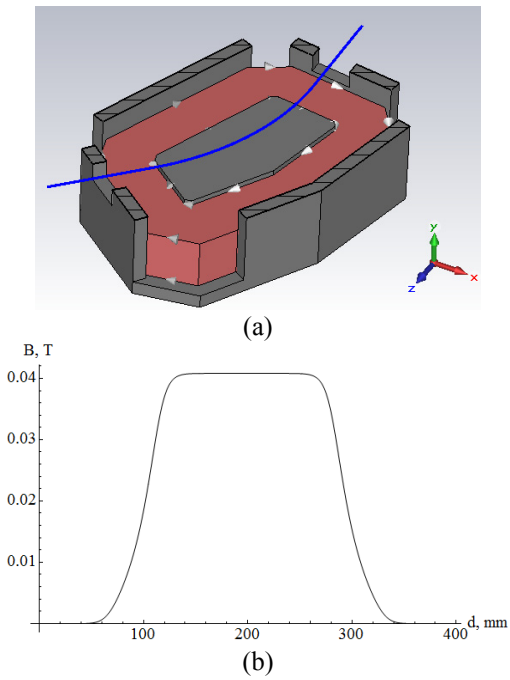

Figure 3: (a) Half of the dipole magnet. (b) Distribution of the magnetic induction along reference trajectory in median plane.

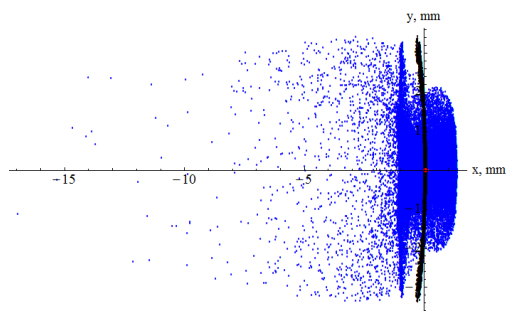

Figure 4: Beams spots on the spectrometer screen: blue points - $\langle p \rangle = 3.060$ MeV/c, $\Delta p = 0.004$ MeV/c, black - $\langle p \rangle = 3.060$ MeV/c, $\Delta p = 0$ MeV/c.

We should note that the field induction for this spectrometer design has to vary from 0.013 T to 0.133 T to bend the beam to 45^0 for the momentum range $1 \leq p \leq 10$ MeV/c. These values, especially the first one, are quite low. So residual magnetization of poles and yoke material, which can change from one switching on to the other, can produce significant contribution to the total field leading to the error in measured beam energy. So we suppose that the spectrometer must include a precise Hall probe to control field level independently of coils current.

SINGLE SHOT PHASE SPACE MEASUREMENT

We also simulated longitudinal phase portrait measurements by spectrometer and TCav [5]. For this purpose we approximated electromagnetic field of the cavity by field of TM_{110} cavity without beam hole:

$$E_r = 0,\ E_\phi = 0,\ E_z = E_0 J_1(kr)\cos\phi,$$
$$B_r = -\frac{E_0}{\omega r} J_1(kr)\sin\phi, \quad (1)$$
$$B_\phi = -\frac{E_0}{c} J_1'(kr)\cos\phi\,, B_z = 0,$$

where ω is angular resonance frequency of the cavity, k - wavenumber, E_0 is amplitude of electric field, c – velocity of light, J_1 – first order Bessel function. The length of cavity was taken to be equal to half wavelength of RF field.

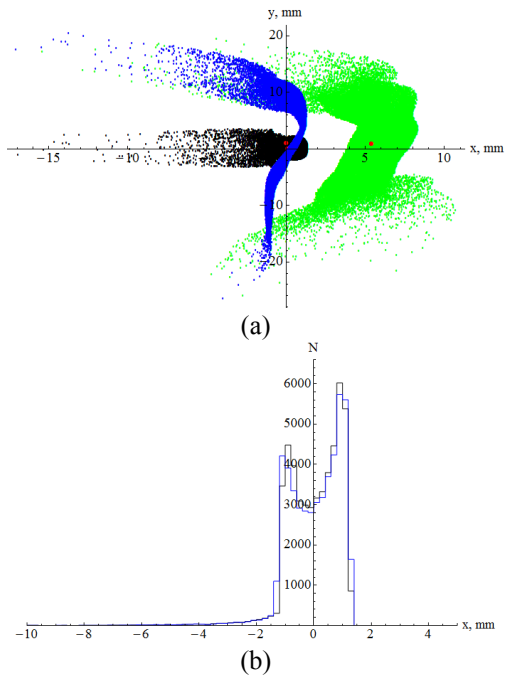

Figure 5: (a) Beams spots on the spectrometer screen: black – TCav was switched off, blue – electric field of cavity was switched off and magnetic field was switched on, green – electric and magnetic fields of cavity were switched on. (b) Beam histograms along x axis.

Figure 5 (a) shows the beam spots at the spectrometer screen for three simulation cases. In each case initial beam had average momentum $\langle p \rangle = 3.060$ MeV/c and momentum spread $\frac{\Delta p}{p} = 0.0013$. In black you can see the distribution at the spectrometer screen without TCav. The green distribution arises if we switch on TCav. It is to see that we get an additional contribution to the energy distribution. This effect comes from the longitudinal

ISBN: 978-3-95450-132-8 doi:10.18429/JACoW-IPAC2014-THPME150

electric field. For a hypothetical TCav with $E_z = 0$ (blue distribution) this effect doesn't exist.

Figure 5 (b) shows the beam histograms along x axis on screen without TCav and for hypothetical TCav. We can see that the magnetic field of the cavity only stretched beam along vertical y axis. When electric field of cavity was switched on, the beam average momentum $\langle p \rangle$ and momentum spread Δp were changed and became equal to $\langle p \rangle = 3.082$ MeV/c and $\frac{\Delta p}{p} = 0.0023$. Thus, non zero length TCav with TM_{110} mode changes beam momentum and momentum spread.

We propose following method to analyze longitudinal phase portrait. We estimate that after TCav electrons change their momentums and coordinates approximately according formulas:

$$y = \frac{2\pi e E_0 \beta}{m_0 \gamma \omega^2}\left(\cos\psi - \frac{\pi}{2}\sin\psi\right),$$
$$p_y = \frac{2\pi e E_0 \beta}{\pi\omega}\sin\psi, \qquad (2)$$
$$p_z = p_{z0} + \frac{2e^2 E_0^2 \beta}{m_0 \gamma \omega^3}\cos\psi\left(\cos\psi - \frac{\pi}{2}\sin\psi\right),$$

where m_0 is electron rest mass, γ – relativistic factor, e – electron charge, ψ – phase of entrance to cavity. Here and further we suppose that electron has entrance coordinate and momentum components: $x_0 = 0$, $y_0 = 0$, $p_{x0} = 0$, $p_{y0} = 0$ and p_{z0}. After TCav electrons pass through drift section, dipole magnet and second drift section. We know transformation matrix M of this system. So we can estimate electron coordinates x_s and y_s on the screen:

$$x_s = M_{16}\frac{p_z - p_{ref}}{p_{ref}}, \qquad (3)$$
$$y_s = M_{33} y + M_{34}\frac{p_y}{p_z},$$

where p_{ref} – reference electron momentum. If we combine Eq. (2) and (3), we can restore electron entrance phase ψ and momentum p_{z0}, i.e. longitudinal phase space distribution, from coordinates x_s and y_s at the screen.

In Fig. 6 we demonstrate operation of this method. Electron beam had average momentum $\langle p \rangle = 3.060$ MeV/c and momentum spread $\frac{\Delta p}{p} = 0.0013$ and passed through TCav and dipole magnet. Beam spot at the screen is shown in Fig. 5 (a) (green) and initial longitudinal phase portrait is shown in Fig. 6 (black). This beam we note as "real" beam. Using method described above we derive blue distribution. Significant difference is due to the fact that in the described method it is assumed that the initial coordinates x, y and momentum components p_x, p_y of all electrons in the beam are equal to 0. And this assumption is not right to real beam. For comparison in Fig. 6 another (red) longitudinal phase portrait is shown. This portrait is result of application of described method to "ideal" beam that as "real" beam had average momentum $\langle p \rangle = 3.060$ MeV/c and momentum spread $\frac{\Delta p}{p} = 0.0013$ and passed through TCav and dipole magnet but had initial coordinates x, y and momentum components p_x, p_y of all beam electrons equal to 0.

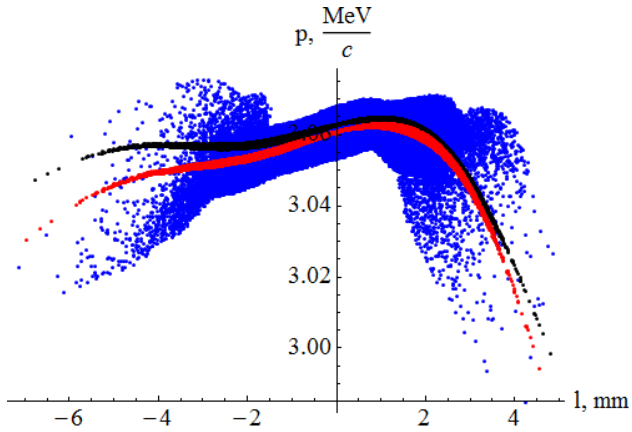

Figure 6: Illustration of method to restore longitudinal phase space distribution: black – portrait of "real" beam, blue – result of method application to "real" beam, red – result of method application to "ideal" beam.

To use the described method, it is necessary to place the additional horizontal collimation slit at the Basic point. As a result it will be possible to obtain a longitudinal portrait without significant widening of energy spread (red phase portrait in Fig. 6).

CONCLUSION

We designed the spectrometer optimized for GunLab and bERLinPro experiments. Also we proposed method to analyze longitudinal phase space distribution.

REFERENCES

[1] J. Voelker et al., "Introducing GunLab a compact test facility for SRF photoinjectors", these proceedings, MOPRI020, IPAC'14, Dresden, Germany (2014).
[2] A. Jankowiak et al., "Conceptual design report BERLinPro", Helmholtz-Zentrum Berlin, Berlin (2012).
[3] CST code, https://www.cst.com
[4] K. Floettmann, ASTRA, A Space charge Tracking Algorithm, http://www.desy.de/~mpyflo
[5] A. Ferrarotto et al., "A novel transverse deflecting cavity for slice diagnostics at BERLinPro", these proceedings, THPME105, IPAC'14, Dresden, Germany (2014).